Dynamic Partitioning of an Aromatic Probe between the Headgroup and Core Regions of Cationic Micelles

Hu Cang, David D. Brace, and M. D. Fayer*

Department of Chemistry, Stanford University, Stanford, California 94305

Received: April 9, 2001; In Final Form: July 10, 2001

Fluorescence lifetime measurements of 2-ethylnaphthalene (2EN) probes in the cationic micelles tetradecyl-trimethylammonium chloride (TTAC), tetradecyl-trimethylammonium bromide (TTAB), dodecyl-trimethyl-ammonium bromide (DTAB), and dodecyl-trimethylammonium chloride (DTAC) demonstrate the close proximity of the 2EN to the Br^- counterions. The fluorescence lifetimes in TTAB and DTAB are much shorter than in TTAC and DTAC because of fluorescence quenching caused by the external heavy atom (Br^-) effect. These results indicate that 2EN resides to a substantial degree in the headgroup region of the micelles. However, detailed analysis of the fluorescence decays shows that the decays are nonexponential in TTAB and DTAB. For micelles with chloride counterions, the fluorescence decays are single exponentials. Fluorescence measurements on nonmicelle solutions with bromide ions are also single exponentials. The results indicate that 2EN is exchanged between the headgroup and the core regions on a short time scale. Analysis of the data with a kinetic model provides information on the faction of the 2EN in the headgroup regions and on the exchange rates. The results show that exchange between the headgroup and the core occurs on a 5 to 10 ns time scale, depending on the micelle. At any given time, ∼80% and ∼50% of the 2EN are found in the headgroup regions of the tetradecyl and dodecyl micelles, respectively.

I. Introduction

Associating probe molecules with micelles is a common technique used to study intramicelle properties, for example, the micelle's microviscosity[1] or the oxygen concentration in the micelle phase.[2] Because of the differences in the properties of the headgroup and core regions of micelles, different types of molecules are expected to locate selectively in the two regions. However, for many common classes of probe molecules, there is still considerable debate about the exact location of probes in micelles. Knowledge of the location of a molecule bound to a micelle is important if the results of measurements on the molecular probe are to be useful. In addition, micelles are valuable in pharmaceutical applications.[3] Therefore, the location of species that are dissolved in micelles can have important practical implications. Furthermore, the concept of "location" may be misleading. As shown below, the location of a probe molecule in a micelle need not be static. Although a molecule, such as 2-ethylnaphthalene, which is studied here, may be found predominantly in the headgroup region, its location is dynamic; it can move between the headgroup and core regions rapidly.

NMR methods have been widely used to study the location of probe molecules in micelles.[4−6] UV spectroscopy has also been used.[7] Most research concludes that aromatic probes prefer the headgroup region in cationic micelles such as dodecyl-trimethylammonium bromide (DTAB). Time dependent fluorescence measurements can also provide useful information about probe environment and location. Naphthalene was found to partition between the aqueous phase and the micelle phase.[5,8,9] (Naphthalene is slightly soluble in water in contrast to 2EN, which is insoluble in water.) Matzinger et al.[10] found aromatic ionic probes 2-(N−Hexadecylamino)-naphthalene-6-sulfonate (HANS) and 2-(N-Decylamino)-naphthalene-6-sulfonate (DANS) are located predominantly in the headgroup region, but a fraction (∼10%, the exact value depending on the molecule and the micelle) reside in the core region of the cationic micelle DTAB and similar micelles. Kowalczyk et al.[11] obtained information from fluorescence measurements on the diffusion of naphthalene in and out of the SDS micelles. Pansu and co-workers[12,13] observed the diffusion of bianthryl probes following optical excitation, which produces a substantial change in structure, from the core to the headgroup region of cetyltrimethylammonium chloride (CTAC) micelles.

In this paper, time dependent fluorescence measurements of 2-ethylnaphthalene (2EN) probes in the cationic micelles DTAB, tetradecyl-trimethylammonium bromide (TTAB), dodecyl-trimethylammonium chloride (DTAC), and tetradecyl-trimethyl-ammonium chloride (TTAC) are reported. The high quality time dependent fluorescence decay data demonstrate that a significant fraction of 2EN probes are located in the headgroup region. The fluorescence decays in the micelles with bromide counterions are short compared to those with chloride counterions. The reduction in the lifetime is caused by the external heavy atom affect.[10] Therefore, the 2EN is located in close proximity to the bromide counterions, which are located near the headgroups. However, careful analysis of the fluorescence decays for the micelles with bromide counterions shows that the decays are nonexponential, while decays for the micelles with chloride counterions are exponential. Data taken on 2EN in bromo containing solutions are exponential as are decays from hydrocarbon solutions. The fluorescence lifetime results were analyzed with kinetic equations describing a dynamic partitioning model. The results yield the exchange rates of 2EN between the headgroup and core regions of the micelles, and the factions of 2EN in the regions. The results indicate that an exchange occurs on a time scale of 5 to 10 ns, depending on the micelle, and that at any given time, ∼80% and ∼50% of the 2EN is found

10.1021/jp0113127 CCC: $20.00 © 2001 American Chemical Society

TABLE 1: Micelle Sample Properties

micelle	cmc (mM)	N_{agg}	[S] (mM)	[M] (mM)
TTAB	3.5	68	114	1.67
TTAC	5.4	65	134	1.40
DTAB	15.4	54	162	2.9
DTAC	16.0	47	243	3.0

in the headgroup regions of the tetradecyl and dodecyl micelles, respectively.

II. Experimental Procedures

A. Materials. TTAC, TTAB, DTAB, tetramethylammonium bromide (TMAB) and 2-ethylnaphthalene were obtained from Aldrich Chemicals. DTAC was obtained from ACROS Organics. All compounds were purchased in the highest available grade. 2EN was selected as the probe molecule for several reasons. Unlike naphthalene, which is slightly soluble in water, 2EN is effectively insoluble in water. Therefore, partitioning or exchange of 2EN between the micelles and water did not enter into the analysis. In addition, 2EN is a liquid at room temperature, and it is easy to purify. 2EN was vacuum distilled before use. Octane, cyclohexane, and 1-bromooctane were obtained from Aldrich Chemicals. Ethylene glycol was obtained from J. T. Baker. DTAB, TTAB, and TTAC were purified by recrystallization from methanol/acetone three times. DTAC were purified by recrystallization from 2-propanol. All organic solvents were checked for fluorescent impurities. Deionized water was vacuum distilled.

The concentration of micelles in solution is calculated using

$$[M] = ([S] - cmc)/N_{agg}$$

[M] is the micelle concentration, [S] is the surfactant concentration, cmc is the critical micelle concentration and N_{agg} is the aggregation number. The concentrations of all surfactant samples are listed in Table 1. The micelle concentrations are kept low enough so that they are in the monodispersed, spherical micelle phase.[14,15]

The chromophore concentrations in the micelle solutions are adjusted so that there is 1 chromophore for every 10 micelles. This ensures that a micelle will contain at most a single chromophore. The chromophore concentration in the organic solvents cyclohexane, octane, and ethylene glycol was 1 mM. Experiments were also conducted with concentrations of 0.1 mM, and the results were the same.

To prevent oxygen quenching of fluorescence lifetimes, all samples containing 2EN were degassed by 10 to 20 cycles of freeze−pump−thaw. Dry N_2 was used to backfill the samples after each pump cycle. The samples were sealed under dry N_2 in fused silica cuvettes. To avoid contamination, the glassware was thoroughly cleaned and nonchromophore samples were checked for fluorescent impurities.

B. Instrumentation. Time-correlated single photon counting (TCSPC) was used to measure the fluorescence decays. The principles of TCSPC were discussed by O′Connor and Phillips.[16] The details of the instrument were described previously.[17] A cavity dumped dye laser generated 640 nm ∼10 ps pulses with an average output power of 20 mW at 823 kHz repetition rate. The output was frequency doubled to 320 nm and used as the excitation pulses. The fluorescence was collected from the front surface of the sample and passed through a subtractive double monochromator to a Hamamatsu microchannel plate detector. The instrument response function was ∼50 ps fwhm. The polarization of the excitation beam was set at the magic angle 54.7° with respect to a polarizer in front of the monochromator.

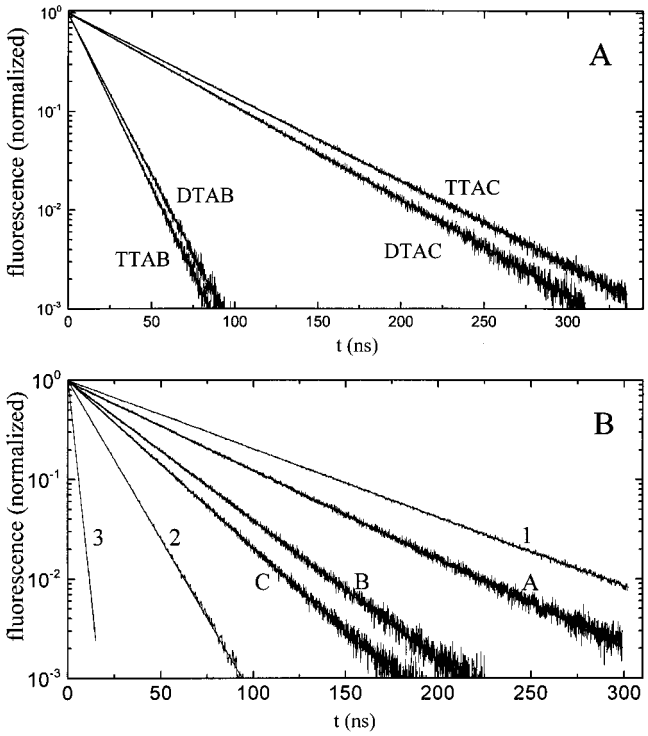

Figure 1. (A) Normalized fluorescence decay curves of 2EN in DTAC, TTAC, DTAB, and TTAB solutions. The decays in micelles with Br^- counterions are substantially faster than the decays in the micelles with Cl^- counterions. (B) 2EN fluorescence decays in ethylene glycol, ethylene glycol/tetramethylammonium bromide (TMAB) solutions and octane/1-bromooctane solutions. As the TMAB concentration is increased, the fluorescence lifetime of 2EN decreases. A. Pure ethylene glycol. B. 0.32 M TMAB. C. 0.43 M TMAB (saturated solution). As the 1-bromooctane concentration is increased, the decays become faster. 1. Pure octane. 2. 0.5 M 1-bromooctane. 3. Pure 1-bromooctane. The data are fit perfectly with single exponentials (see Tables 2 and 3).

The monochromator wavelength was set at 337 nm for all samples with a bandwidth wide enough to collect essentially the entire fluorescence band of 2EN. All measurements were carried out at room temperature. The time to amplitude converter (TAC) and the multichannel analyzer (MCA) were calibrated using an EG&G Ortec 462 time calibrator. 20 000 to 30 000 counts were collected for each decay.

A program based on Levenberg−Marquardt method[18] was used to analyze the fluorescence decays. In most instances, the points were weighted as 1 over the square root of the amplitude. The residuals shown below are weighted. The model decay functions were convolved with experimentally measured instrument response. However, because the fwhm of the TCSPC instrument response is 50 ps and all of the fluorescence decay times were ∼2 ns or longer, the instrument response convolution has a negligible effect.

III. Experimental Results

Figure 1(A) shows the normalized fluorescence decay curves of 2EN in DTAC, TTAC, DTAB, and TTAB solutions. Initially, we are only concerned with the qualitative difference between the micelles with Cl^- counterions and those with Br^- counterions. The lines through the data are single-exponential fits. As discussed in detail below, the decays in TTAC and DTAC are perfect single exponentials, but the decays in TTAB and DTAB are not. The important point here is that the decays in micelles with Br^- counterions are substantially faster (i.e., 13.4 and 12.3 ns for DTAB and TTAB, respectively) than the decays in the

TABLE 2: 2-Ethylnaphthalene Fluorescence Lifetimes in Different Concentrations of TMAB/Ethylene Glycol Solutions

	0.43 M TMAB	0.32 M TMAB	ethylene glycol
single exp decay time, γ (ns)	25.8 ± 0.04	30.9 ± 0.1	48.5 ± 0.02

Error bars − 99% confidence interval.

micelles with Cl^- counterions (i.e., 45.9 and 50.6 ns for DTAC and TTAC, respectively).

The significantly shorter fluorescence decay time for 2EN in DTAB and TTAB micelle solutions as compared to 2EN in TTAC and DTAC solutions is a result of the proximity of the Br^- to the 2EN chromophore.[10] It is well-established that the bromide counterion in CTAB micelles can quench the fluorescence of aromatic chromophores.[2,10,19−22] The nature of the quenching mechanism is still a matter of debate and probably depends on the chromophore. Two possible mechanisms for the quenching process have been proposed, namely, quenching by the external heavy atom effect[20,21] and quenching by electron transfer (charge-transfer complexes).[23−25] It is also known that the chloride counterion in CTAC does not significantly quench the fluorescence of aromatic compounds. For 2EN, the quenching mechanism is almost certainly the external heavy atom effect. The susceptibility of naphthalene to the external heavy atom effect is well documented.[26,27] Because the heavy atom effect goes as $\sim Z^4$, Cl has little affect in most cases, but Br has a substantial affect.

Matzinger et al. performed very detailed studies of the fluorescence lifetimes of HANS and DANS in CTAB, TTAB, DTAB, CTAC, TTAC, and DTAC.[10] They studied the influences of counterions, ionic strength in solution as well as other micelle and solution properties on the lifetime and orientational relaxation of the chromophores. In the Br^- counterion micelles, they observed a biexponential decay of the fluorescence, consisting of a fast component with ~90% of the intensity and a slow component with ~10% of the intensity. The fast component lifetime was ~5 ns and the slow component lifetime was ~20 ns. The lifetimes and percentages varied somewhat depending on the chromophore and the micelle. In the Cl^- counterion micelles, they observed the same slow component, but the fast component became a factor of 2 slower, that is, ~10 ns. Comprehensive studies in solutions with various ions and measurements of orientational relaxation led to the conclusion that 90% of the chromophores are located in the headgroup region near the counterions and 10% are located in the core, far from the counterions. When the counterion is changed from Br^- to Cl^-, the external heavy atom affect is turned off, and the lifetimes become substantially longer. However, the lifetime in the polar headgroup region is shorter than in the nonpolar core even in the absence of the heavy ion effect.

The data presented in Figure 1 can be interpreted in terms of the prior work. It suggests that 2EN is located in the headgroup regions of the micelles. In DTAB and TTAB, the 2EN fluorescence lifetimes are fast compared to the lifetimes in DTAC and TTAC because the 2EN is located near the Br^-. As additional tests of the quenching of the 2EN fluorescence by Br^- or Br atoms, 2EN fluorescence decays were measured in several bromine containing solutions. Tetramethylammonium bromide (TMAB) was used as a model of the micelle headgroups. 2EN is not soluble in water. Therefore, 2EN fluorescence decays were recorded in ethylene glycol and ethylene glycol/TMAB solutions. The results are shown in Figure 1B (curves labeled A, B, and C) and listed in Table 2. As the TMAB concentration is increased, the fluorescence lifetime of 2EN decreases. As will be discussed further below, each of these decays is described perfectly by a single exponential. In the solution saturated with TMAB (0.43 M), the lifetime of 2EN is 25.8 ns, which is still longer than 13.4 ns, the observed lifetime of 2EN in DTAB.

TABLE 3: 2-Ethylnaphthalene Fluorescence Lifetimes in Organic Solvents

	cyclohexane	octane	0.5 M 1-bromooctane in octane	1-bromooctane
single exp decay time, γ (ns)	59.9 ± 0.01	63.1 ± 0.01	15.7 ± 0.01	2.5 ± 0.0

Error bars − 99% confidence interval.

2EN fluorescence decays in octane/1-bromooctane solutions were also investigated. The results are shown in Figure 1B (curves labeled 1, 2, and 3) and Table 3. The lifetime decreases as the 1-bromooctane concentration is increased. For a 1-bromooctane concentration of 0.5 M, the lifetime of 2EN is 15.1 ns, close to the lifetime of 2EN in DTAB micelle solution. Again, the fluorescence decay for all solutions shown in Figure 1B and listed in Table 3 fit over the full range of times to a single-exponential decay.

From the information presented above, an apparent conclusion can be drawn. The 2EN resides close to the Br^- counterions. When the counterion is changed from Br^- to Cl^-, the decays change from ~12−13 ns t*o* ~46−51 ns. Removing the bromide counterion, eliminates (or greatly reduces) the external heavy atom affect, and the rate of fluorescence decay decreases. However, there is a difference between the decays observed here and the previous results on DANS and HANS in the same micelles. For Hans and DANS in DTAB and TTAB, the fluorescence decay was biexponential, with the long components having decay constants that are approximately the same as the lifetimes measured in pure hydrocarbon solvents. The amplitude of the long hydrocarbon like decay constant, ~10%, gives the percentage of the chromophores located in the core regions of the micelles. 2EN in DTAB and TTAB does not display a long fluorescence component that is comparable to its lifetime in hydrocarbon solvents. From this result, one might conclude that 2EN is located exclusively in the headgroup region with a negligible percentage in the core.

The fluorescence decays observed in ethylene glycol and in ethylene glycol with various concentrations of TMAB, in octane and in octane with various concentrations of 1-bromooctane, in pure 1-bromooctane, in cyclohexane, in DTAC, and in TTAC, are all perfect single exponentials. Figure 2 shows a fluorescence decay of 2EN in DTAC. The main part of the figure is an ln plot with the best single exponential fit. The inset shows the decay of the first 12 ns as a linear plot and the line through the data is the same single exponential fit. Plots of the residuals (B) and the autocorrelation of the residuals (C) are shown below the data. The residuals fluctuate randomly about zero. The autocorrelation of the residuals is a single spike at 0, demonstrating that the single exponential fit describes the data extremely well.[16,28]

Figure 3 shows a fluorescence decay of 2EN in DTAB. The main part of the figure is an ln plot with the best single exponential fit for the long time portion of the data. As in Figure 1, this single exponential appears to describe the entire time range of the data. However, the inset shows the short time data on a linear plot with the single exponential curve. Unlike the data in Figure 2, there is a deviation from a single exponential

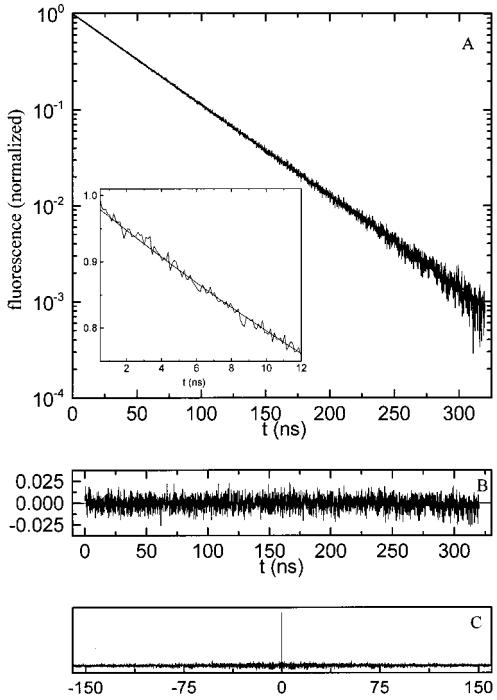

Figure 2. Fluorescence decay of 2EN in DTAC. The main part of the figure is an ln plot with the best single exponential fit. The inset shows the decay of the first 12 ns on a linear plot, and the line through the data is the same single exponential fit. Plots of the residuals (B) and the autocorrelation of the residuals (C) are shown below the data. The residuals fluctuate randomly about zero. The autocorrelation of the residuals is a single spike at 0, demonstrating that the single exponential fit describes the data extremely well.

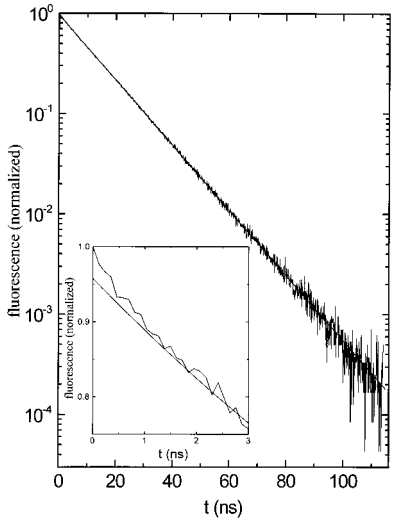

Figure 3. Fluorescence decay of 2EN in DTAB. The main part of the figure is an ln plot with the best single-exponential fit for the long time portion of the data. The single exponential appears to describe the entire time range of the data. However, the inset shows the short time data on a linear plot with the single exponential. The data deviates from a single exponential (see Figure 4).

at short time. Figure 4 shows two sets of residuals and two sets of the autocorrelations of the residuals. The upper two panels are for the best single exponential fit. The residuals (A) clearly oscillate above and below the line, in contrast to the residuals for DTAC shown in Figure 2. The autocorrelation of the residuals (B) is not a single spike. It has significant breadth, in contrast to the autocorrelation of the residuals for DTAC shown in Figure 2. The fluorescence decay of 2EN in DTAB is not a

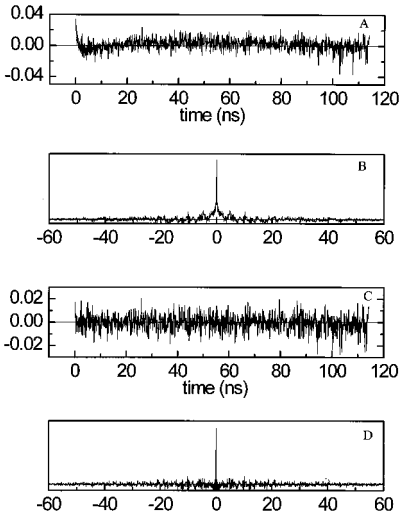

Figure 4. Two sets of residuals and two sets of the autocorrelations of the residuals for the data in Figure 3. The upper panels are for the single exponential fit. The residuals (A) clearly oscillate above and below the line, in contrast to the residuals for DTAC shown in Figure 2. The autocorrelation of the residuals (B) is not a single spike. It has significant breadth, in contrast to the autocorrelation of the residuals for DTAC shown in Figure 2. C and D are the residuals and the autocorrelation of the residuals for a biexponential fit (eq 1). The residuals are random about 0, and the autocorrelation of the residuals is a single spike at 0. The DTAB decay is a biexponential.

TABLE 4: 2-Ethylnaphthalene Fluorescence Lifetimes in the Micelle Solutions

	A_1	A_2	γ_1 (ns)	γ_2 (ns)
TTAB	0.9776 ± 0.0021	0.0224 ± 0.0019	12.3 ± 0.02	3.1 ± 0.3
TTAC	1		50.6 ± 0.1	
DTAB	0.9685 ± 0.0007	0.0315 ± 0.0015	13.4 ± 0.01	1.6 ± 0.09
DTAC	1		45.9 ± 0.02	

Error bars − 99% confidence interval.

single-exponential decay. The TTAB data displays the same nonexponential behavior.

The decay data for DTAB and TTAB were fit to a biexponential,

$$F(t) = A_1 \exp(-t/\gamma_1) + A_2 \exp(-t/\gamma_2) \qquad (1)$$

where γ_1 and γ_2 are the decay times of the two components of the observed biexponential decays. The lower panels in Figure 4 are the residuals and the autocorrelation of the residuals for a biexponential fit to the DTAB data. For the biexponential fit, the residuals (C) are random about the line and the autocorrelation of the residuals (D) is a single spike. A biexponential fit to the TTAB data also shows the same excellent agreement with the data. The lack of a trend in the residuals and the delta function spike in the autocorrelation of the residuals is an effective way of checking the quality of the fits.[16,28] The results show that there is no systematic deviation between the fits and the data. Therefore, the fluorescence decays in DTAB and TTAB are well described by a biexponential, whereas in all of the other samples the decays are single exponentials. The results of the biexponential and single-exponential fits for fluorescence decays for the four micelles are given in Table 4. The lifetimes for all of the data given in Tables 2−4 have error bars that are the 99% confidence interval.

The second component of the biexponential is very fast, 1.6 ns for DTAB and 3.1 ns for TTAB. This is not the same type of behavior observed by Matzinger et al. for HANS and DANS in these micelles.[10] In their study, the long component was

comparable to the decay for the chromophores in hydrocarbon solvents. Here, the slower decay is fast compared to the decay in hydrocarbons and there is an even faster component. As discussed above, the time scale of the slower decay is caused by the external heavy atom affect. The particular value is consistent with a relatively high local concentration of Br^- counterions. The fast component is not caused by a distribution of distances between the 2EN and the Br^-. In the solutions of 2EN with various concentrations of TMAB or 1-bromooctane, single exponentials was always observed, even though there is a distribution of distances. The 2EN is interacting with a number of Br^- at once, and fairly rapid diffusion of the 2EN and the ions will average out the distance distribution on the ns time scale. Recent determinations of the diffusion constants in the headgroup regions of DTAB and TTAB of a molecule (dimethyl-1-naphthylamine) similar to 2EN show that the 2EN diffusion constant is $\sim$15 Å^2/ns.[29] Diffusion in the headgroup region of the micelles is considerably faster than in the ethylene glycol/TMAB solutions. Therefore, an inhomogeneous distribution of quenching rates caused by the external heavy atom effect is not responsible for the biexponential decay. A contribution to fluorescence decay from 2EN in the aqueous phase is ruled out because a water sample with the same path length as the micelle samples saturated with 2EN shows no fluorescence with the TCSPC apparatus. In addition, the single exponential decays observed for 2EN in DTAC and TTAC micelle solutions demonstrate that the additional fast decay component in DTAB and TTAB does not come from 2EN dissolved in water.

IV. Dynamic Partition Model

Matzinger et al. described the partitioning of chromophores between the headgroup and core regions of the micelles and related the ratio of preexponential factors of the biexponential decay function to the population partition ratio between the two regions. This is referred to as the "Static Partition Model". As discussed above, this model cannot account for the biexponential decay for 2EN in DTAB and TTAB.

NMR studies[4,5,7,30−32] show that a substantial fraction of aromatic chromophores are located in the headgroup regions of cationic micelles. Kowalcayk et al.[11] found that naphthalene tends to exchange between the aqueous phase and the sodium dodecyl sulfate (SDS) micelle phase. After a careful study of the dynamics, they concluded that the exchange process could affect the time dependent fluorescence decay, producing nonexponential decays. Because 2EN is insoluble in water, exchange between the water and the micelle does not occur in the systems studied here. However, the naphthalene/SDS results indicate the role that exchange between two media can have on fluorescence decays.

On the basis of the data and analysis presented in section III and the previous studies involving chromophore diffusion, we propose that although a substantial fraction of 2EN is located in the headgroup region, some is located in the core. However, contrary to the static partition model, there is fast exchange of 2EN probes between these two regions. 2EN is dynamically partitioned between the headgroup region and the core region. This "Dynamic Partition Model" can explain all of the observations presented in section III, provide information on the exchange rate between the headgroup and core, and provide the faction of chromophores found in each region.

Birks[33] and Kowalcayk et al.[11] have addressed the problem theoretically. Here, a simpler model is used that is sufficient to analyze the data. 2EN is partitioned between the two regions, with subscript 1 corresponding to the headgroup region and 2 corresponding to the core region. The first peak in the absorption spectrum of the S_0 to S_1 transition (the 0−0 transition) is a single, relatively narrow feature, $\sim$3 nm fwhm. The laser bandwidth, which is not transform limited, is sufficiently broad to excite the band. It is assumed that the absorption for 2EN in the headgroup and core are both contained within this band, and 2EN in either region is excited with equal probability. In detecting the fluorescence, virtually the entire fluorescence spectrum is observed. Therefore, a possible difference in the emission spectra between 2EN in the headgroup and core regions does not come into play. Immediately after excitation, the number of excited 2EN in two regions are $N_1(0)$ and $N_2(0)$. These numbers reflect the ground-state partitioning of 2EN between the two regions. In the absence of exchange, the time dependent fluorescence decay rates for the two regions are $k_1 = 1/\tau_1$ and $k_2 = 1/\tau_2$, where τ_1 and τ_2 are the two fluorescence lifetimes that would be observed if static partition occurred. There is fast exchange of excited 2EN between the two regions. The exchange rates between headgroup and core and core and headgroup are described by constants. k_{12} is the rate constant for 2EN migration from the headgroup region to the core region, and k_{21} is the rate constant for 2EN migration from the core region to the headgroup region. The inverse of the exchange rates, $1/k_{12}$ and $1/k_{21}$, describes the time an excited 2EN stays in headgroup region and in the core region, respectively.

The rate equations for the population of 2EN in two regions are

$$\frac{d}{dt}N_1 = -(k_1 + k_{12})N_1 + k_{21}N_2$$

$$\frac{d}{dt}N_2 = k_{12}N_1 - (k_2 + k_{21})N_2 \qquad (2)$$

The solutions can be written in matrix form

$$\begin{pmatrix} N_1(t) \\ N_2(t) \end{pmatrix} = \exp\left[\begin{pmatrix} -(k_1 + k_{12}) & k_{21} \\ k_{12} & -(k_2 + k_{21}) \end{pmatrix} t\right] \begin{pmatrix} N_1(0) \\ N_2(0) \end{pmatrix} \qquad (3)$$

with $N_1(0) + N_2(0) = 1$. The eigenvalues of matrix in eq 3 are the two decay rate constants for the observed biexponential decay.[33] Although the solutions to eq 3 are not difficult to obtain, the expressions are quite long. Therefore, they are given in Appendix A. The total fluorescence detected as a function of time is the sum of the time dependent fluorescence from the two regions because the detection is broadband

$$F(t) \propto k_f N_1(t) + k_f N_2(t) \propto N_1(t) + N_2(t) \qquad (4)$$

k_f is the intrinsic radiative decay rate constant, which is assumed to be the same in both regions. The observed decay rate constants depend on the intrinsic total decay constants (radiative plus nonradiative), k_1 and k_2, and on the exchange rate constants, k_{12} and k_{21}. The preexponential factors (i.e., the amplitude of each decay component, A_1 and A_2 in Table 4) depend on the initial populations and the exchange rate constants.

The exchange rates for 2EN in DTAC and DTAB are assumed to be equal. The exchange rates in TTAB and TTAC are also assumed to be equal, but not necessarily the same as in DTAC and DTAB. Br^- is more polarizable than Cl^-. Therefore, it could interact more strongly with 2EN, and the dynamic partitioning of 2EN between the headgroup region and the core could be influenced by the counterion. The data analysis given below is consistent with the assumption that the exchange rates are independent of the counterion. The 2EN fluorescence lifetime, τ_2, in the core regions of all four micelles is taken to

be the same. The cores of the micelles are composed of the tails of the DTAB, TTAB, DTAC, and TTAC molecules, which are alkyl chains. To have a value for τ_2, we employ the fluorescence lifetime of 2EN in octane (63.1 ns). The static lifetime, τ_1, is different for TTAB and DTAB vs TTAC and DTAC because of the heavy atom effects. τ_1 may also depend on the size of the micelle because the surface areas, effective concentration of bromide counterions, and the amount of water penetration into the headgroup region will vary with size. Therefore, for all micelles, $\tau_2 = 63.1$ ns, the exchange rate constants depend on the size of the micelle but not the counterion, and τ_1 depends on both the counterion and the size of the micelle.

Equation 4 with the solutions given in Appendix A was used to reproduce the data. In all cases, the results given in Table 4 could be reproduced precisely. In principle, there are 6 parameters that go into the calculations, but not all of these are free parameters. As stated above, τ_2 was fixed at 63.1 ns for all micelles. $N_1(0)$ and $N_2(0)$ are the steady-state fractions of 2EN in regions 1 (headgroup) and 2 (core) when 2EN is in its ground electronic state. k_{12} and k_{21}, the exchange rates between the regions, are for excited 2EN molecules because only excited 2EN is observed in the fluorescence experiments. However, the properties of 2EN in the ground and first excited singlet state should not differ much. 2EN is nonpolar in both the ground and excited states. There is no major change in structure or dipole moment caused by electronic excitation. The excited state will be somewhat more polarizable than the ground state, which could possibly make a small difference in the partitioning. We assume that k_{12} and k_{21} are almost identical in the ground and excited states. Then

$$\frac{N_1(0)}{N_2(0)} \cong \frac{k_{21}}{k_{12}} \tag{5}$$

Furthermore, all of the parameters for the bromide and chloride micelles with the same surfactant must be the same except for τ_1. τ_1 is the lifetime in the headgroup region in the absence of exchange. It should be significantly faster with the bromide counterions because of the external heavy atom affect. These constraints place severe restrictions on the parameters that can be used to describe the data. For a given value of τ_1, it is possible to find values of $N_1(0)$ and $N_2(0)$ and k_{12} and k_{21} that will fit the data. However, the condition in eq 5 is violated for all but a very narrow range of τ_1 values. The parameters for the tetradecyl and dodecyl micelles need not be the same since the headgroup properties of these micelles differ (see below).

For each micelle, the biexponential or single-exponential decay constants and the amplitudes of the decay components (see Table 4) are reproduced. Figure 5 displays the data for 2EN in DTAC as well as several calculated curves. The line through the data is the full calculation, $N_1 + N_2$. It reproduces the observed single-exponential decay. Also shown are the individual N_1 and N_2 calculated curves. Inset A shows the short time portion of the data, the calculated $N_1 + N_2$ curve through the data, and the individual $N_1(t)$ and $N_2(t)$ curves. The decays for both the headgroup and core regions are nonexponential immediately after time zero. The excited state population of 2EN in the core region increases initially, whereas the population in the headgroup region decays at a faster rate than the long time rate. After ~20 ns, the decays of N_1 and N_2 go to the same rate; the exchange process has brought the entire system to dynamic equilibrium. Although N_1 and N_2 are nonexponential decays, the sum of N_1 and N_2 fits the single-exponential decay

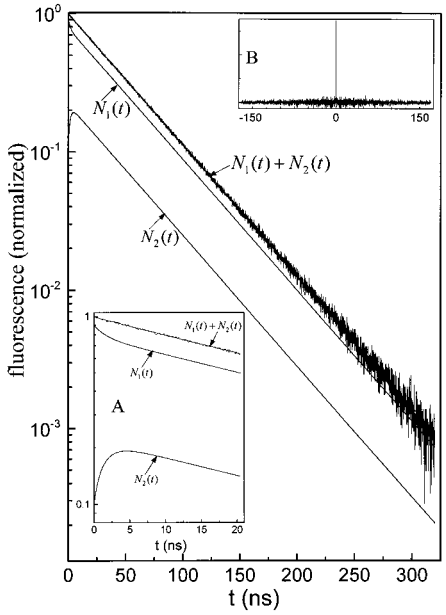

Figure 5. 2EN in DTAC fluorescence decay data and several calculated curves. The line through the data is $N_1 + N_2$. It reproduces the observed single-exponential decay. Also shown are the individual N_1 and N_2 calculated curves. Inset A. The short time portion of the data, the calculated $N_1 + N_2$ curve through the data, and the individual $N_1(t)$ and $N_2(t)$ curves. Although N_1 and N_2 are nonexponential, the sum of N_1 and N_2 fits the single-exponential decay well. Inset B. The autocorrelation of the residuals is a single spike confirming the agreement between the calculation and the data.

well, as can be seen in inset A that shows the short time portion of the data and the total calculated curve. The agreement between the calculation and the data is demonstrated by the autocorrelation of the residuals shown in inset B, which is a single spike.

The biexponential fluorescence decay of 2EN in DTAB and calculated curves are shown in Figure 6. The line through the data is the sum $N_1 + N_2$. The individual N_1 and N_2 curves are also shown. Inset A shows the short time portion of the data and the calculated curve $N_1 + N_2$ through the data as well as the individual N_1 and N_2 curves. The agreement between the calculation and the nonexponential data is demonstrated by the autocorrelation of the residuals shown in inset B, which is a single spike.

Table 5 presents the results of using the Dynamic Partition Model to fit the data. r and r^* are defined as

$$r = \frac{N_1(0)}{N_2(2)} \tag{6}$$

$$r^* = \frac{k_{21}}{k_{12}} \tag{7}$$

The first two rows of the table are for TTAB and TTAC. As required, the two experimental curves are reproduced with all of the parameters the same except for the τ_1 values. The τ_1 in TTAB is shorter than in TTAC because of the external heavy atom affect. In TTAC, the observed value of the apparent single-exponential decay, $\gamma_1 = 50.6$ ns (Table 4) is between the τ_1 and τ_2 values. Because τ_1 and τ_2 are quite similar, the nonexponential nature of the TTAC decay is not detectable. The results indicate that ~80% of 2EN ($N_1(0)$) is found in the headgroup regions of TTAC and TTAB. In TTAB, the observed value of the dominant exponential decay component of the

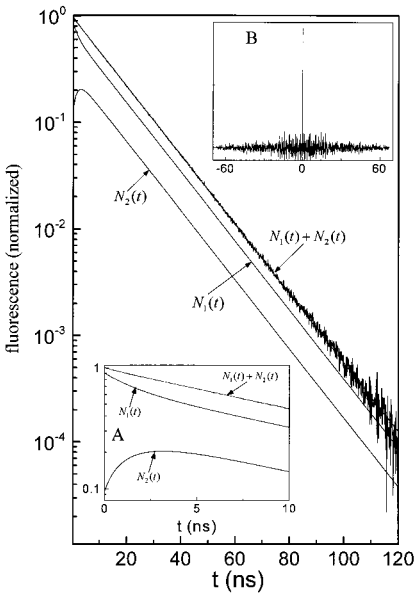

Figure 6. Biexponential fluorescence decay of 2EN in DTAB and calculated curves. The line through the data is the sum $N_1 + N_2$. The individual N_1 and N_2 curves are also shown. Inset A shows the short time portion of the data and the calculated curve $N_1 + N_2$ through the data as well as the individual N_1 and N_2 curves. The agreement between the calculation and the data is demonstrated by the autocorrelation of the residuals shown in inset B, which is a single spike.

biexponential, $\gamma_1 = 12.3$ ns (Table 4) is also between the τ_1 and τ_2 values. However, because τ_1 and τ_2 are very different, the exchange between the headgroup and core produces an observable nonexponential decay with $\gamma_2 = 3.1$ ns (Table 4). r and r^* are identical within experimental error, as required under the assumption that the properties of 2EN do not change significantly in the excited state. Given a headgroup diffusion constant of ~15 Å^2/ns,[29] there is certainly enough time for the 2EN to diffuse the required distance to move between the headgroup and core regions of the micelle.

The last two lines of Table 5 are for DTAB and DTAC. The two experimental curves are reproduced with all parameters the same except for the τ_1 values. Again, the τ_1 for DTAB is shorter than in DTAC because of the external heavy atom affect. In DTAC, the observed value of the apparent single-exponential decay, $\gamma_1 = 45.9$ ns (Table 4) is between the τ_1 and τ_2 values. Because τ_1 and τ_2 are quite similar, the nonexponential nature of the DTAC decay is not detectable. The results indicate that ~50% of 2EN ($N_1(0)$) is found in the headgroup regions of DTAC and DTAB. In DTAB, the observed value of the dominant exponential decay component of the biexponential, $\gamma_1 = 13.4$ ns (Table 4) is also between the τ_1 and τ_2 values. Because τ_1 and τ_2 are very different, the exchange between the headgroup and core produce an observable nonexponential decay with $\gamma_2 = 1.6$ ns (Table 4). r and r^* are the same within experimental error as required under the assumption that the properties of 2EN do not change significantly in the excited state.

The τ_1 values for TTAB and DTAB differ as do the τ_1 values for TTAC and DTAC. The intrinsic lifetimes in the headgroup regions of the dodecyl micelles are faster than those in the tetradecyl micelles. The difference could arise because of the difference in the headgroup structures of the two micelles. Neutron scattering experiments on DTAB and TTAB reveal that the headgroup structures of the two micelles differ significantly.[34] In TTAB, water penetrates into the headgroup region to a depth of ~2.5 carbons, whereas in DTAB water penetrates in ~4 carbons. This difference in the extent of water present in the headgroup region presumably reflects the difference in size of the micelles. The smaller DTAB should have a more open headgroup structure than TTAB. The difference in structure and the increased dielectric constant and polarity of the DTAB headgroup region compared to TTAB can affect the lifetime. The lifetime of 2EN in ethylene glycol solution is 48.5 ns (Table 2), which is substantially shorter than the 63.1 ns lifetime in octane (Table 3). In TTAB and DTAB, the headgroup region lifetimes are quite short, but they are still long compared to the 2EN lifetime of 2.5 ns measured in pure 1-bromooctane (Table 3). The lifetimes are consistent with a high local Br^- concentration but not as high as in pure 1-bromooctane.

The $N_1(0)$ values given in Table 5 show that ~80% of the 2EN is in the headgroup region of the tetradecyl micelles, whereas the value is ~50% for the dodecyl micelles. The difference in the partitioning between the headgroup and core can also be attributed to the difference in the headgroup structure of the two types of micelles. 2EN is essentially insoluble in water. Using the time correlated single photon counting apparatus, no fluorescence could be detected from a saturated solution of 2EN in water. The fact that aromatic molecules tend to locate in the headgroup region of trimethylammonium alkyl micelles is due to the high polarizability of 2EN. The somewhat polar anisotropic environment of the headgroup region, which is mix of hydrocarbon with some water, will induce a dipole in the 2EN. The dipole-induced dipole interaction is attractive, making 2EN quite soluble in the headgroup region. 2EN is also very soluble in hydrocarbons. The increased water content of the headgroup region may be responsible for the reduction in the percentage of 2EN in the dodecyl micelles. The water content may be so great in the dodecyl micelles, particularly near the surface, that it reduces the 2EN solubility. It is interesting to note that although the k_{12} rate constants (headgroup to core) are different for the tetradecyl and dodecyl micelles, the k_{21} rate constants are essentially identical. The difference in the k_{12} rate constants reflects the different structures of the headgroup regions of the two types of micelles. The similarity in the k_{21} rate constants indicates the similarity in the core regions.

One important consideration that needs to be kept in mind is the nature of the observable that leads to the determination of the dynamic partitioning between the headgroup and the core of the micelles. The information comes from quenching of the fluorescence by the external heavy atom affect in the bromide counterion micelles. In these experiments, the headgroup region and the core region really means proximity to the Br^- counterions and away from the Br^- counterions. 2EN is somewhat smaller than the size of the headgroup region. It can diffuse rapidly in the headgroup region.[29] In 1 ns time scale, which is fast compared to the intrinsic lifetimes obtained for the headgroup regions (τ_1 values in Table 5), 2EN can move sufficiently far to repeatedly sample the micelle surface and the Br^-. Therefore, equating the two regions in the kinetic model with the headgroup and cores regions is reasonable. Another consideration is that the kinetic model uses rate constants in to and out of the core. A more detailed model could include diffusion of the 2EN in the core region, which could lead to a much more complicated form for the kinetic equations. The data do not warrant a more complex model because the current model is capable of reproducing the data. The excellent agreement between the model and the data may indicate that even when 2EN is in the core, it remains approximately at the headgroup-core interface.

TABLE 5: Dynamic Partition Model Results

	τ_1 (ns)	τ_2 (ns)[a]	$N_1(0)$	$N_2(0)$	$1/k_{12}$ (ns)	$1/k_{21}$ (ns)	r	r^a
TTAB	9.5 ± 0.5	63.1	0.79 ± 0.04	0.21 ± 0.04	17.2 ± 0.4	4.5 ± 0.4	3.8 ± 0.2	3.9 ± 0.4
TTAC	48.0 ± 0.5	63.1	0.79 ± 0.04	0.21 ± 0.04	17.2 ± 0.4	4.5 ± 0.4	3.8 ± 0.2	3.9 ± 0.4
DTAB	6.5 ± 0.5	63.1	0.54 ± 0.04	0.46 ± 0.04	4.4 ± 0.4	4.4 ± 0.4	1.2 ± 0.1	1.0 ± 0.2
DTAC	35.8 ± 0.5	63.1	0.54 ± 0.04	0.46 ± 0.04	4.4 ± 0.4	4.4 ± 0.4	1.2 ± 0.1	1.0 ± 0.2

[a] Assumed to be the same as the decay in octane. Error bars were estimated based on the errors in the measurements, the variation in the quality of the fits with the change in the parameters, and estimations of possible error introduced by the assumptions of the model.

V. Concluding Remarks

Time-resolved fluorescence measurements were used to examine the dynamic partitioning of 2-ethylnaphthalene between the headgroup and core regions of DTAB, DTAC, TTAB and TTAC micelles. A kinetic model is used to analyze the fluorescence data and obtain the fraction of 2EN found in the headgroup and core regions and to determine the rate constants for exchange between the two regions. It is found that in TTAB and TTAC, 80% of the 2EN is located in the headgroup region, while in DTAB and DTAC, 50% is in the headgroup region. It is proposed that the difference in the factions is caused by differences in the structures of the headgroup regions of the tetradecyl and dodecyl micelles.

The dynamic partition model used to analyze the data describes the 2EN molecules as constantly exchanging between the headgroup and the core regions. When the 2EN are in the headgroup region of Br^- counterion micelles, they have a fast lifetime because of the external heavy atom affect. When they are in the core, they have a long lifetime associated with a hydrocarbon environment. The large difference in lifetimes in the two environments produces a fast ($\sim$2 ns) component in the observed fluorescence decay caused by the exchange between the two regions. In the micelles with Cl^- counterions, the lifetimes in the headgroup and the core are similar. Although exchange still occurs and the decay is in principle nonexponential, calculations show that the decay will appear to be exponential, consistent with the data. Analysis of the data yields the rate constant for exchange from the headgroup to core and core to headgroup regions (Table 5). The exchange rates are fast compared to the intrinsic lifetimes in the core. The fast exchange combined with the large difference in lifetimes between the core and headgroup regions in the Br^- counterion micelles makes the exchange observable in the fluorescence decays. In the Cl^- counterion micelles, even though the experimental fluorescence decay is a single exponential, the decay constant is not the intrinsic lifetime of 2EN in either the headgroup or core regions. It is a weighted average. In systems in which the intrinsic lifetimes are relatively fast,[10] although exchange may be occurring, exchange will not be manifested in the functional form of the fluorescence decays. The net result is that partitioning of probe molecules and other species between the headgroup and core regions of micelles can be dynamic. The fraction of probes in each region is determined by the steady-state dynamics of the system.

Acknowledgment. This work was supported by the Department of Energy, Office of Basic Energy Sciences (Grant DE-FG03-84ER13251) and by the National Science Foundation, Division of Materials Research (Grant DMR-0088942).

Appendix A

The solutions of eqs 2 can be written formally as

$$\begin{pmatrix} N_1(t) \\ N_2(t) \end{pmatrix} = \exp\left[\begin{pmatrix} -(k_1 + k_{12}) & k_{21} \\ k_{12} & -(k_2 + k_{21}) \end{pmatrix} t\right] \begin{pmatrix} N_1(0) \\ N_2(0) \end{pmatrix} \quad \text{(A1)}$$

The total fluorescence, $F(t)$, is proportional to the sum of fluorescence from the two regions (headgroup -1; core -2)

$$F(t) \propto N_1(t) + N_2(t) \quad \text{(A2)}$$

K and Δ are defined as

$$K = k_1 + k_{12} + k_2 + k_{21}$$
$$\Delta = k_{12}k_2 + k_{21}k_1 + k_1k_2 \quad \text{(A3)}$$

Each solution is a biexponential with the exponential decay constants, $\lambda_\pm$, given by

$$\lambda_\pm = \frac{1}{2}(K \pm \sqrt{K^2 - 4\Delta}) \quad \text{(A4)}$$

The solution are

$$N_1(t) = \frac{1}{2}\exp(-\lambda_+ t)\left[N_1(0)\left(1 + \frac{(k_1 + k_{12} - k_2 - k_{21})}{\sqrt{K^2 - 4\Delta}}\right) - \frac{2k_{21}}{\sqrt{K^2 - 4\Delta}}N_2(0)\right] + \frac{1}{2}\exp(-\lambda_- t)\left[N_1(0)\left(1 + \frac{(-k_1 - k_{12} + k_2 + k_{21})}{\sqrt{K^2 - 4\Delta}}\right) + \frac{2k_{21}}{\sqrt{K^2 - 4\Delta}}N_2(0)\right] \quad \text{(A5)}$$

$$N_2(t) = \frac{1}{2}\exp(-\lambda_+ t)\left[N_2(0)\left(1 + \frac{(k_2 + k_{21} - k_2 - k_{21})}{\sqrt{K^2 - 4\Delta}}\right) - \frac{2k_{12}}{\sqrt{K^2 - 4\Delta}}N_1(0)\right] + \frac{1}{2}\exp(-\lambda_- t)\left[N_2(0)\left(1 + \frac{(-k_2 - k_{21} + k_1 + k_{12})}{\sqrt{K^2 - 4\Delta}}\right) + \frac{2k_{12}}{\sqrt{K^2 - 4\Delta}}N_1(0)\right] \quad \text{(A6)}$$

Then, the total fluorescence, $F(t)$, is

$$F(t) \propto N_1(t) + N_2(t) \propto \frac{1}{2}\exp(-\lambda_+ t)\left[N_1(0)\frac{(k_1 - k_{12} - k_2 - k_{21})}{\sqrt{K^2 - 4\Delta}} + N_2(0)\frac{(k_2 - k_{21} - k_{12} - k_1)}{\sqrt{K^2 - 4\Delta}} + 1\right] + \frac{1}{2}\exp(-\lambda_- t)\left[N_1(0)\frac{(k_{12} + k_{21} + k_2 - k_1)}{\sqrt{K^2 - 4\Delta}} + N_2(0)\frac{(k_{12} + k_{21} + k_1 - k_2)}{\sqrt{K^2 - 4\Delta}} + 1\right] \quad \text{(A7)}$$

References and Notes

(1) Shinitzky, M.; Dianoux, A.-C.; Gitler, C.; Weber, G. *Biochemistry* **1971**, *10*, 2106.

(2) Hautala, R. R.; Schore, N. E.; Turro, N. J. *J. Am. Chem. Soc.* **1973**, *95*, 5508.
(3) Maestro, M. *J. Mol. Liq.* **1989**, *42*, 71.
(4) Hawrylak, B. E.; Marangoni, D. G. *Can. J. Chem.* **1999**, *77*, 1241.
(5) Wasylishen, R. E.; Kwak, J. C. T.; Gao, Z.; Verpoorte, E.; MacDonald, J. B.; Dickson, R. M. *Can. J. Chem.* **1991**, *69*, 822.
(6) Ulmius, J.; Lindman, B.; Lindblom, G.; Drakenberg, T. *J. Colloid Inter. Sci.* **1978**, *65*, 88.
(7) Heindl, A.; Strnad, J.; Kohler, H.-H. *J. Phys. Chem.* **1993**, *97*, 742.
(8) Hatuala, R. R.; Turro, N. J. *Mol. Photochem.* **1972**, *4*, 93.
(9) Almgren, M.; Grieser, F.; Powell, J. R.; Thomas, J. K. *J. Am. Chem. Soc.* **1979**, *101*, 279.
(10) Matzinger, S.; Hussey, D. M.; Fayer, M. D. *J. Phys. Chem.* **1998**, *102*, 7216.
(11) Kowalczyk, A. A.; Vecer, J.; Hodgson, B. W.; Keene, J. P.; Dale, R. E. *Langmuir* **1996**, *12*, 4358.
(12) Pansu, R. B.; Yoshihara, K. *J. Phys. Chem.* **1991**, *95*, 10 123.
(13) Laguitton-Pasquier, H.; Pansu, R.; Chauvet, J. P.; Pernot, P.; Collet, A.; Faure, J. *Langmuir* **1997**, 19 077.
(14) Lindman, B. Structural Aspects of Surfactant Micellar Systems. In *Surfactants*; Tadros, T. F., Ed.; Academic Press: Orlando, 1984; p 83.
(15) Reiss-Husson, F.; Luzzati, V. *J. Phys. Chem.* **1964**, *68*, 3504.
(16) O'Conner, D. V.; Phillips, D. *Time-Correlated Single Photon Counting*; Academic Press: London, 1984.
(17) Stein, A. D.; Peterson, K. A.; Fayer, M. D. *J. Chem. Phys.* **1990**, *92*, 5622.
(18) Constantinides, A.; Mostoufi, N. *Numerical Methods for Chemical Engineers with MATHLAB Applications*; Prentice Hall: 1999.
(19) Burrows, H. D.; Formosinho, S. J.; Paiva, M. F. J. R.; Rasburn, J. *J. Photochem.* **1980**, *12*, 285.
(20) Wolff, T. *Ber. Bunsen-Ges. Phys. Chem.* **1982**, *86*, 1132.
(21) Meling, H.; Wolff, T.; Bünau, G. v. *Ber. Bunsen-Ges. Phys. Chem.* **1988**, *92*, 200.
(22) Sarpal, R. S.; Dogra, S. K. *J. Photochem. Photobiol. A* **1995**, *88*, 147.
(23) Brooks, C. A. G.; Davis, K. M. C. *J. Chem. Soc., Faraday Trans. 2* **1972**, 1649.
(24) Bendig, J.; Siegmund, M.; Helm, S. *Adv. Mol. Relax. Int. Proc.* **1979**, *14*, 121.
(25) Mac, M.; Najbar, J.; Phillips, D.; Smith, T. A. *J. Chem. Soc., Faraday Trans.* **1992**, *88*, 3001.
(26) McGlynn, S. P. *Chem. Rev.* **1958**, *58*, 1113.
(27) McGlynn, S. P.; Azumi, T.; Kinoshita, M. *Molecular Spectroscopy of the Triplet State*; Prentice Hall: Englewood Cliffs, NJ, 1969; Vol. Chapter 8.
(28) Lakowicz, J. R. *Principles of Fluorescence Spectroscopy*; Kluwer Academic/Plenum: New York, 1999.
(29) Tavernier, H. L.; Laine, F.; Fayer, M. D. *J. Phys. Chem.* **2001**, accepted.
(30) Ganesh, K. N.; Mltra, P.; Balasubramanlan, D. *J. Phys. Chem.* **1982**, *86*, 4291.
(31) Lianos, P.; Viriot, M.-L.; Zana, R. *J. Phys. Chem.* **1984**, *88*, 1098.
(32) Duns, G. J.; Reeves, L. W.; Yang, D. W.; Williams, D. S. *J. Colloid Inter. Sci.* **1995**, *173*, 261.
(33) Birks, J. B. *Photophysics of Aromatic Molecules*; Wiley-Interscience: London, 1970.
(34) Berr, S.; Jones, R. R. M.; Johnson, J. S. *J. Phys. Chem.* **1992**, *96*, 5611.